



**HAL**  
open science

## **Anti-Inflammatory effect of anti-TNF- $\alpha$ SiRNA cationic phosphorus dendrimer nanocomplexes administered intranasally in a murine acute lung injury model**

Adam Bohr, N. Tsapis, I. Andreana, A. Chamarat, C. Foged, C. Delomenie, M. Noiray, Nabil El brahmi, Jean Pierre Majoral, Serge Mignani, et al.

### **► To cite this version:**

Adam Bohr, N. Tsapis, I. Andreana, A. Chamarat, C. Foged, et al.. Anti-Inflammatory effect of anti-TNF- $\alpha$  SiRNA cationic phosphorus dendrimer nanocomplexes administered intranasally in a murine acute lung injury model. *Biomacromolecules*, 2017, 18 (8), pp.2379-2388. 10.1021/acs.biomac.7b00572 . hal-01945636

**HAL Id: hal-01945636**

**<https://hal.science/hal-01945636>**

Submitted on 24 Oct 2019

**HAL** is a multi-disciplinary open access archive for the deposit and dissemination of scientific research documents, whether they are published or not. The documents may come from teaching and research institutions in France or abroad, or from public or private research centers.

L'archive ouverte pluridisciplinaire **HAL**, est destinée au dépôt et à la diffusion de documents scientifiques de niveau recherche, publiés ou non, émanant des établissements d'enseignement et de recherche français ou étrangers, des laboratoires publics ou privés.

**ANTI-INFLAMMATORY EFFECT OF ANTI-TNF- $\alpha$  siRNA CATIONIC PHOSPHOROUS  
DENDRIMERS NANOCOMPLEXES ADMINISTERED INTRANASALLY IN A MURINE  
ACUTE LUNG INJURY MODEL**

5 Adam Bohr<sup>1,2</sup>, Nicolas Tsapis<sup>1</sup>, Ilaria Andreana<sup>1</sup>, Anais Chamarat<sup>1</sup>, Camilla Foged<sup>2</sup>, Claudine  
Delomenie<sup>3</sup>, Magali Noiray<sup>1</sup>, Nabil El Brahmi<sup>4,5</sup>, Jean-Pierre Majoral<sup>4,5</sup>, Serge Mignani<sup>6</sup> and Elias  
Fattal<sup>1\*</sup>

<sup>1</sup> Institut Galien Paris-Sud, CNRS, Univ. Paris-Sud, Université Paris-Saclay, 92296 Châtenay-  
Malabry, France.

10 <sup>2</sup> Department of Pharmacy, Faculty of Health and Medical Sciences, University of Copenhagen,  
Universitetsparken 2, 2100 Copenhagen, Denmark

<sup>3</sup> UMS IPSIT - US 31 INSERM - UMS 3679 CNRS - Université Paris-Sud – 5, rue Jean-Baptiste  
Clément 92296 CHATENAY-MALABRY, France.

15 <sup>4</sup> Laboratoire de Chimie de Coordination, CNRS, 205 route de Narbonne F-31077 Toulouse Cedex  
4, France

<sup>5</sup> Université de Toulouse, UPS, INPT, Toulouse, France

<sup>6</sup> Laboratoire de Chimie et de Biochimie pharmacologiques et toxicologiques, CNRS UMR 860,  
Université Paris Descartes, PRES Sorbonne Paris Cité, 45 rue des Saints Pères, 75006, Paris, France

20 \* Corresponding author:

Elias Fattal, Ph.D.; Châtenay-Malabry, France

Tel.: 0033146835568

E-mail : elias.fattal@u-psud.fr

## 25 **Abstract**

Inflammation is an essential component of many lung diseases, including asthma, chronic obstructive pulmonary disease (COPD) or acute lung injury. Our purpose was to design efficient carriers for lung delivery of small interfering RNA (siRNA) targeting tumor necrosis factor (TNF- $\alpha$ ) in an acute lung injury model. To achieve this goal, two different types of phosphorus-based dendrimers with either pyrrolidinium or morpholinium as terminal protonated amino groups were selected for their better biocompatibility compared to other dendrimers. Dendriplexes containing pyrrolidinium surface groups demonstrated a stronger siRNA complexation, a higher cellular uptake and enhanced *in vitro* silencing efficiency of TNF- $\alpha$  in the lipopolysaccharide (LPS)-activated mouse macrophage cell line RAW264.7, compared to morpholinium-containing dendriplexes. The better performance of the pyrrolidinium dendriplexes was attributed to their higher pKa value leading to a stronger siRNA complexation and improved protection against enzymatic degradation resulting in a higher cellular uptake. The superior silencing effect of the pyrrolidinium dendriplexes, compared to non-complexed siRNA, was confirmed *in vivo* in an LPS-induced murine model of short term acute lung injury upon lung delivery via nasal administration. These data suggest that phosphorous dendriplexes have a strong potential in lung delivery of siRNA for treating inflammatory lung diseases.

### **Keywords**

siRNA; TNF- $\alpha$ ; lung inflammation; dendriplex; phosphorous dendrimer; transfection efficiency, LPS

45

## 1 Introduction

Inflammation is an essential component of many lung diseases such as asthma, chronic obstructive pulmonary disease (COPD) or acute lung injury (ALI)<sup>1,2</sup>. ALI and the acute respiratory distress syndrome (ARDS) are common causes of intensive care mortality<sup>3</sup>. In ALI, resident and recruited alveolar macrophages play a key role in initiating and maintaining pulmonary inflammation<sup>4</sup>. Alveolar macrophages from ALI patients have increased baseline and stimulated secretory levels of proinflammatory proteins, including certain cytokines and chemokines<sup>5</sup>. Of the numerous cytokines, tumor necrosis factor (TNF- $\alpha$ ) is believed to play a key role in the inflammation process<sup>6</sup>. Current medicinal treatment of the inflammation involves anti-inflammatory drugs, such as glucocorticoids, which quite often result in systemic drug exposure and undesired side effects<sup>7</sup>. Treatment based on small interfering RNA (siRNA) may therefore provide a more specific and less toxic therapy in which the inflammatory pathways leading to TNF- $\alpha$  secretion can be targeted. One of the major obstacles limiting the use of siRNA as a drug is their low permeation across cell membranes due to their unfavorable physicochemical properties (high molecular weight and positive charge) and their poor stability in biological fluids. Thus, synthetic carriers, including nanocarriers using cationic lipids or cationic polymers *e.g.*, polyethylenimine (PEI) or chitosan, have been designed for lung delivery of siRNA<sup>8,9</sup> as they protect them from enzymatic degradation and further facilitate their transmembrane delivery and release into the cytoplasm<sup>10</sup>. In this work, we have applied a new family of dendrimers as siRNA carriers. Dendrimers are synthetic polymers characterized by a branched structure and a globular shape with high monodispersity and vast opportunities for surface tailoring as well as their ability to condense nucleic acids into nanoparticles<sup>11,12</sup>. Indeed, dendrimers have been shown to be efficient siRNA delivery systems *in vitro* and *in vivo* in several studies, where mostly the commercially available polyamidoamine (PAMAM) dendrimers have been used<sup>13,14</sup>. However, in very preliminary *in vitro* experiments, phosphorous dendrimers have been shown to be more efficient in cellular delivery of siRNA compared to PAMAM dendrimers<sup>15</sup>. Phosphorous dendrimers have a backbone consisting of aminothiophosphates at every branching point. In addition, they possess intrinsic properties that are the easy regioselective functionalization of the core, the possibility to play with the hydrophilicity/hydrophobicity of the surface and of the core, the interior being hydrophobic, their biocompatibility and biodegradability as well as high thermal stability<sup>16-18</sup>. Further, it has been shown that phosphorous dendrimers may exhibit anti-inflammatory properties<sup>19,20</sup>. Indeed, incubation of a polyanionic phosphorous dendrimer with activated monocytes resulted in the up-regulation of the expression of several anti-inflammatory cytokines, including interleukin (IL)-10

80 <sup>19-21</sup>. The local administration to the lungs of dendriplexes carrying an antiTNF- $\alpha$  siRNA can be considered to exert its effect directly on the inflamed tissue. Interactions with serum proteins that degrade siRNA after intravenous administration is mitigated as serum is absent on the air-side of the lung and nuclease activity is comparably low <sup>9,22,23</sup>.

85 For this study, two different cationic, phosphorous dendrimers of generation 3 (G3) were synthesized, functionalized with either cationic pyrrolidinium or morpholinium surface groups. These surface groups are secondary amines, which have both been considered for their excellent binding properties versus nucleic acids <sup>24,25</sup>. The synthesized dendrimers were investigated as transfection agents for the delivery of siRNA directed against TNF- $\alpha$ , and the resulting dendriplexes were characterized and their performance assessed. An activated mouse macrophage cell line and a murine acute lung injury model were used for biological assessment of the prepared siRNA  
90 formulations.

## 2 Experimental Section

### 2.1 Materials

Phosphorous dendrimers were synthesized and characterized by  $^1\text{H}$ ,  $^{13}\text{C}$ , and  $^{31}\text{P}$  NMR. The  
95 phosphorus dendrimer of generation 3 (1G3) bearing 24 terminal  $\text{P}(\text{S})\text{Cl}_2$  was synthesized as  
previously described<sup>26</sup>. Grafting of amino pyrrolidine or aminomorpholine was conducted as  
reported for the grafting of other diamines<sup>27</sup> and leads to dendrimers bearing 48 terminal cationic  
pyrrolidinium groups (DP) or 48 morpholinium groups (DM) (figure 1). Dicer substrate asymmetric  
duplex siRNA directed against  $\text{TNF-}\alpha$ <sup>14</sup> was provided by Integrated DNA Technologies Inc. (IDT,  
100 Coralville, IA, USA) as dried, purified and desalted duplexes. The  $\text{TNF-}\alpha$  siRNA consisted of the  
following sequences:

Sense 5'-pGUCUCAGCCUCUUCUCAUUCCUGct-3',

Antisense 5'-AGCAGGAAUGAGAAAGAGGCUGAGACAU-3', where the lower case letters  
indicate 2'-deoxyribonucleotides, underlined capital letters represent 2'-O-methylribonucleotides  
105 and p is a phosphate residue (Mw 17,047 Da). Negative control sequences of siRNA (scrambled)  
were acquired from Eurogentec (Eurogentec, Angers, France). The exact sequence of the negative  
control siRNA was not disclosed by the supplier. Fluorescent dicer substrate siRNA labeled with  
the dye TYE<sup>TM</sup> 665 was also provided by IDT with a sequence directed against luciferase:

Sense 5'-pGGUUCCUGGAACAAUUGCUUUUAca-3',

110 Antisense 5'-UGUAAAAGCAAUUGUUCCAGGAACCAG-3'.

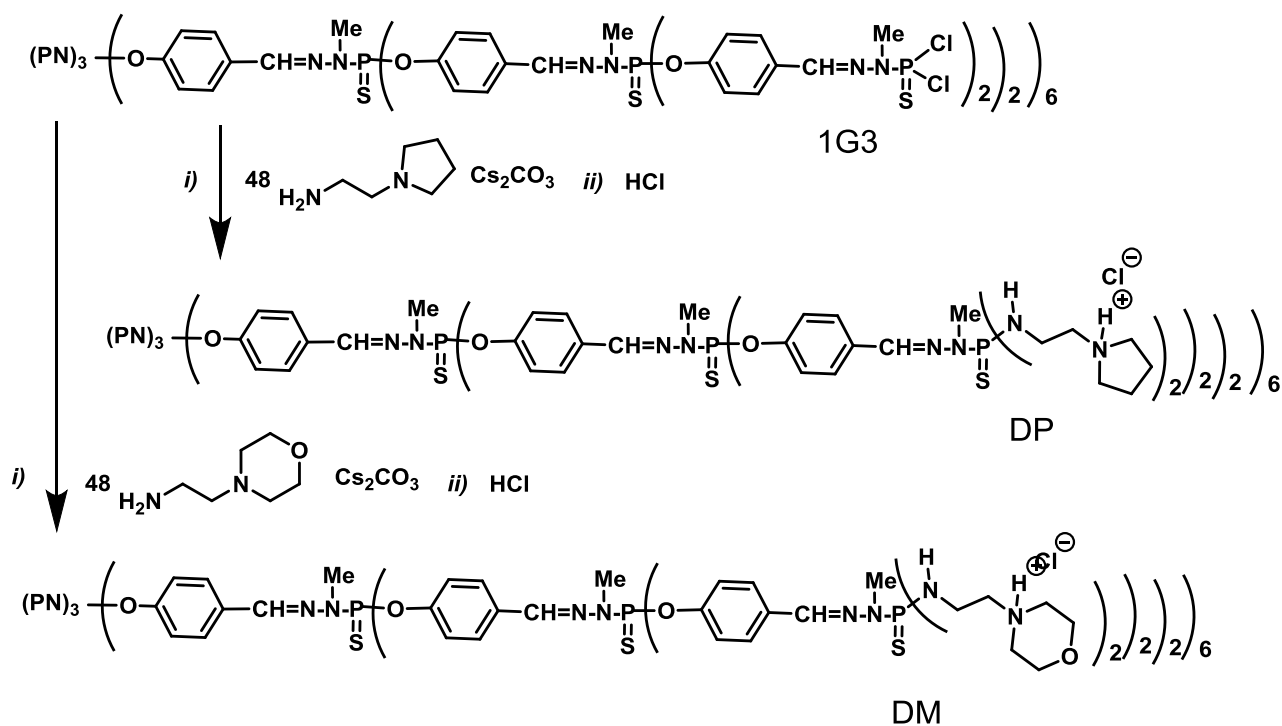


Figure 1. Synthesis and chemical structures of cationic phosphorus dendrimers of generation 3: DP (pyrrolidinium end groups) and DM (morpholinium end groups).

115 RNAse-free diethyl pyrocarbonate (DEPC)-treated water was used for dilutions, buffers and all solutions containing siRNA and dendrimers. The duplexes were re-annealed in duplex buffer consisting of 30 mM 4-(2-hydroxyethyl)-piperazine-1-ethanesulfonic acid (HEPES) and 100 mM potassium acetate prior to any formulation, as recommended by the supplier. All experiments were performed at 25 °C in 10 mM HEPES buffer, pH 7.4 unless otherwise stated. Primers for PCR

120 (Supplementary material, Table S1) were provided by Eurofins MWG Operon (Ebersberg, DE). Lipopolysaccharide (LPS) ( $\gamma$ -irradiated, <1% protein) was obtained from Sigma-Aldrich (St Quentin Fallavier, France), All additional chemicals used were obtained commercially and were of analytical grade.

## 2.2 Acid-base titration

125 The pKa value of each dendrimer was determined after titration. Each dendrimer was dissolved in a 30 mL aqueous solution at a 0.2 mg/mL concentration. The solution was then adjusted to a pH

6

value of 10 using 1 M NaOH, and the pH was measured using a pH meter (Mettler Toledo, Viroflay, France). The solution was then titrated using 1 M HCl in 2  $\mu$ l volume increments down to a pH value of 2 according to the volume of HCl added. From these curves the pKa value was  
130 estimated.

### 2.3 Size and zeta potential measurements

The average particle size (z-average) and polydispersity index (PDI) of the dendrimers were measured by dynamic light scattering (DLS), and the surface charge was assessed by zeta potential analysis (laser-Doppler electrophoresis). Measurements were performed using a Zetasizer Nano ZS  
135 (Malvern Instruments, Worcestershire, United-Kingdom) equipped with a 633 nm laser and 173° detection optics. Dendrimer solutions were prepared at 5.6  $\mu$ M in 10 mM HEPES buffer and a volume of 1 ml was added to the cuvette for measurements. The Malvern DTS v.6.10 software (Malvern Instruments) was used for data acquisition and analysis, and a zeta potential transfer standard ( $-50 \pm 5$  mV, Malvern Instruments) was used to verify the performance of the instrument.

### 140 2.4 Preparation of dendriplexes

All dendriplexes were prepared at a nitrogen-to-phosphate (N/P) ratio (the molar charge ratio between the cationic dendrimer and the anionic siRNA) of 5, 10 or 20, respectively in 10 mM HEPES buffer. In brief, the dendrimer and siRNA solutions were prepared separately in a total volume of 100  $\mu$ l, and 20  $\mu$ l dendrimer solution was added to 80  $\mu$ l of siRNA solution, followed by  
145 vortex mixing. The mixture was left at room temperature for 10 min to allow the complexes to form. The final concentrations of the mixtures were 5  $\mu$ M for siRNA and 28, 56 112  $\mu$ M for the dendrimers at N/P ratios of 5, 10, and 20, respectively. Further adjustment of the concentration was obtained by subsequently diluting in 10 mM HEPES buffer to obtain lower concentrations and by using filter centrifugation for up-concentrating the samples. Amicon Ultra-0.5 mL centrifuge tubes

150 (Thermo-Fisher, Villebon, FR) were used to centrifuge dendriplex dispersions at 11,740 g for 20 min.

## 2.5 Characterization of dendriplexes

The z-average, polydispersity index (PDI) and the zeta potential of the dendriplexes were measured as described above for dendrimers. Measurements were performed on diluted samples at 500 nM  
155 and 2.8  $\mu$ M siRNA and dendrimer, respectively. All samples were prepared in triplicate (n=3) and for each sample, a minimum of three measurements were performed. Gel electrophoresis was performed to assess the binding of siRNA to the dendrimers as dendriplexes. A total amount of 0.1 nmol siRNA was used per well and the electrophoresis was carried out using 1% (w/v) agarose gels (Promega, Madison, WI, USA). The gels were run at 100 V for 20 min in Tris-borate-EDTA (TBE)  
160 buffer (pH 8.2) supplemented with 5  $\mu$ L of 2.5 mg/mL ethidium bromide, and the siRNA bands were visualized using a MF-ChemiBIS gel imaging system (DNR Bio-Imaging Systems, Jerusalem, Israel).

## 2.6 Cell culture

The mouse macrophage cell line RAW264.7 was acquired from American Type Culture Collection  
165 (ATCC), and was used at an unspecified passage number in all cell-based experiments. The cells were cultured using Dulbecco's Modified Eagle's Medium (DMEM) (Sigma Aldrich, St. Louis, MO, USA) supplemented with 10% (v/v) fetal bovine serum (PAA Laboratories, Pasching, Austria), 100 U/ml penicillin, and 100  $\mu$ g/ml streptomycin. The cells were incubated in an atmosphere of 5% CO<sub>2</sub> and 95% O<sub>2</sub> at 37 °C and sub-cultured twice a week by scraping the cells  
170 from the culture flask and re-suspending them in fresh culture medium. The cells were used at 80% confluence between passages 5-10.

## 2.7 Cell viability

The viability of the RAW264.7 cells was measured using the 3-(4,5-dimethylthiazol-2-yl)-2,5-diphenyltetrazolium bromide (MTT) assay. Cells were detached from the surface of culture flasks, pooled, counted, adjusted to the right concentration, and seeded in 96-well plates at a density of  $8 \times 10^3$  cells per well and left overnight. Subsequently, they were incubated with dendriplexes (N/P ratio of 5) at different concentrations for 24 h and the medium was replaced with fresh medium. For each well, 10  $\mu$ l of MTT-solution [5mg/ml in phosphate-buffered saline (PBS), pH 7.4] was added to 100  $\mu$ l of cell culture medium. The plate was incubated for 2 h at 37 °C to allow the transformation of MTT to formazan crystals. The medium was then removed, and 200  $\mu$ l of dimethylsulfoxide was added to each well to dissolve the MTT formazan crystals. Absorbance was spectrophotometrically detected at a wavelength of 570 nm using a microplate reader (FLUOstar OPTIMA, BMG labtech, Champigny-sur-Marne, France). The viability of the cells was calculated as percentage by comparing the absorbance from cell suspensions exposed to dendriplex samples with those from corresponding untreated control cell suspensions. The half-maximal inhibitory concentration (IC<sub>50</sub>) was determined based on the dose-response curve using linear regression and estimated from the fitted line.

## 2.8 Cell uptake

Flow cytometry and fluorescence microscopy were employed to assess the cellular siRNA uptake and intracellular distribution in RAW264.7 cells. For flow cytometry studies, the cells were cultured in 12-well plates in full culture medium at a density of  $5 \times 10^5$  cells per well. The cells were treated with fluorescent siRNA, either non-complexed or in dendriplexes (N/P ratio of 5) at a concentration of 100 nM fluorescent siRNA for 0.5-4 h before resuspension and analysis by flow cytometry using an Accuri C6 (BD biosciences, Franklin Lakes, NJ, USA). These measurements were used to determine the relative uptake, the ratio between the mean fluorescence intensity (MFI) of the treated

samples, and the non-treated negative control, expressed in arbitrary units. For fluorescence microscopy, cells were cultured in chambered coverslips,  $\mu$ -Slide 8 well (Ibidi, Planegg, Germany), at a density of  $5 \times 10^4$  cells per well. The cells were treated with fluorescent siRNA, either non-complexed or as dendriplexes (N/P ratio of 5) at a concentration of 100 nM fluorescent siRNA for 4 h and subsequently washed with PBS and fixed using 4% (v/v) paraformaldehyde. Microscopy images were captured at a 63x magnification with a Zeiss LSM 510 (Carl Zeiss, Jena, DE) fluorescence microscope equipped with a 1 mW helium-neon laser and a plan-apochromat 63X objective lens (numerical aperture 1.40, oil immersion). Differential interferential contrast (DIC) images were collected simultaneously. The TYE™ 665 dye was excited using a 633 nm laser illumination and collected with a 650 nm long pass emission filter. The pinhole was set at 1.0 Airy unit (0.8  $\mu$ m optical slice thickness). Twelve bit numerical images were acquired with LSM 510 software version 3.2 (Carl Zeiss).

## 2.9 Cell transfection

Transfection experiments were performed essentially as previously described<sup>14</sup>. In brief, cells were seeded in 6-well culture plates at a density of  $1 \times 10^6$  cells per well in full culture medium and left overnight. The dendriplexes were prepared as described above (N/P ratio of 5) and 100  $\mu$ l dendriplex suspension was added to each well at different dilutions to achieve final siRNA concentrations of 6, 12, 25, 50 and 100 nM, respectively, in the wells, and incubated for 24 h. Three hours prior to harvesting, 100  $\mu$ l PBS containing LPS was added to each well to obtain a final LPS concentration of 5 ng/ml. Positive controls for inflammation response were not treated with siRNA or dendrimer but were treated with LPS while negative controls were incubated with PBS. At harvesting, the culture medium was removed from the wells and the cells were washed with PBS and subsequently 1 ml cold TRIzol (Thermo Fisher, Villebon-sur-Yvette, France) was added to each well, and the cells were loosened by scraping. The contents of each well was mixed by pipetting, transferred to centrifuge tubes and kept on ice.

RNA extraction was performed from the TRIzol-suspended cell homogenates following the instructions of the protocol provided with TRIzol reagent. The total RNA content of the extract samples was quantified using a UV spectrophotometer, Biomate 3 (Thermo Fisher) with a TrayCell fiber-optic ultra-micro cell (Hellma Analytics, Paris, France) and quality control of the RNA samples was performed with a RNA LabChip, using an Agilent 2100 Bioanalyzer (Agilent, Santa Clara, CA, USA). Reverse transcription of 1 µg RNA samples was done using a mixture of primers applying an iScript cDNA Synthesis Kit (Biorad, Hercules, CA, USA). The cDNA samples were diluted 1:10 in RNase-free water and stored at -80°C. All RNA samples showed a 260/280 ratio between 2.0-2.2 and an RNA integrity number (RIN) number between 9 and 10.

The knockdown of TNF- $\alpha$  mRNA was assessed by real time reverse transcription polymerase chain reaction (RT-PCR) essentially as previously described <sup>14</sup>. All PCR reactions were performed in duplicate in a total reaction volume of 20 µl using 10 µl of SsoAdvanced Universal SYBR Green Supermix (Biorad, Hercules, CA, USA), 5 µl cDNA working solution (1:10 dilution) and 0.5 µM of forward and reverse primers (Table ST1, supplementary material). Real-time PCR was performed using a C1000 Thermal Cycler instrument with a CFX96 Real-Time System (Biorad) with the following cycling conditions: An initial denaturation step at 95 °C for 5 min, followed by 35 cycles of denaturation at 95 °C for 10 s, annealing at 60 °C for 10 s, and elongation at 72 °C for 10 s. The CFX manager software 3.0 (Biorad) was used for crossing point (CP) analysis, and the values were normalized against the average of the two reference genes, glucuronidase b (GUSb) and ribosomal protein, large P2 (RPLP2). These reference genes were chosen from a screening test of eight reference candidates, which showed that the optimal number of reference targets is two or three (geNorm V < 0.15) where good reference target stability is achieved. Gene knockdown data is presented as the relative gene expression compared to the positive control (LPS-treated cells).

## **2.10 *In vivo* studies**

### **2.10.1 *Mice***

Experiments were conducted according to the European rules (86/609/EEC and 2010/63/EU) and the Principles of Laboratory Animal Care and national French legislation (Decree No. 2013-118 of February 1, 2013). All techniques/procedures were refined to provide for maximal comfort and minimal stress to the animals. Mice were housed in groups of four with access to water and food *ad*  
250 *libitum* and kept at constant temperature (19-22°C) and relative humidity (45-65%). Female CD-1 mice were purchased from Envigo (Gannat, France), and all experiments were performed using mice at the age of 6 to 8 weeks.

### ***2.10.2 Lung inflammation model***

A widely used protocol for acute LPS-induced lung inflammation<sup>28-30</sup> was adjusted for CD-1 mice.  
255 The mice were anesthetized by intraperitoneal (i.p.) injection of 200 µl Ketamine (3.5 mg/ml)/Xylazine solution (5 mg/ml), and the animals were monitored until disappearance of the plantar reflex. Using a pipette, the LPS solution (3.2 mg/kg) was administered to the mice by nasal administration (1.2 µl LPS solution/g of mouse weight) by placing the mice on their backs and allowing them to inhale the solution through the nostrils. Subsequently, the mice were allowed to  
260 wake up and were monitored over the next days. For bronchoalveolar lavage (BAL), the mice were euthanized via an overdose of pentobarbital (i.p. injection of 200 µl 20 mg/ml pentobarbital solution), and the trachea was exposed from an incision and cannulated with a 22-gauge catheter (BD biosciences). Subsequently, BAL was performed by flushing the lungs with seven times 0.3 ml  
265 counting/differentiation, whereas the last five lavages were used only for cell counting/differentiation. The BAL was centrifuged at 400g for 10 min, the supernatant was stored at -20 °C for protein quantification, and the pellets were pooled and resuspended in fresh PBS.

### ***2. 10.3 Experimental design***

270 Mice were dosed with the siRNA as a prophylactic treatment prior to inducing inflammation in their lungs (Figure 2). Dendriplexes (N/P ratio of 5) were administered via nasal administration as  
12

described for the LPS administration. They were given at an siRNA concentration of 2.0 mg/kg in an average volume of 30  $\mu$ l 24 h prior to administration of LPS. The mice were assessed 4 and 72 h after the LPS challenge, and a minimum of five mice were included in each treatment group. They were dosed either with siRNA targeting TNF- $\alpha$  or non-coding scrambled siRNA (SCR). Positive controls were pretreated with PBS, and were subsequently dosed with LPS. Negative controls were pretreated with PBS and were subsequently given PBS.

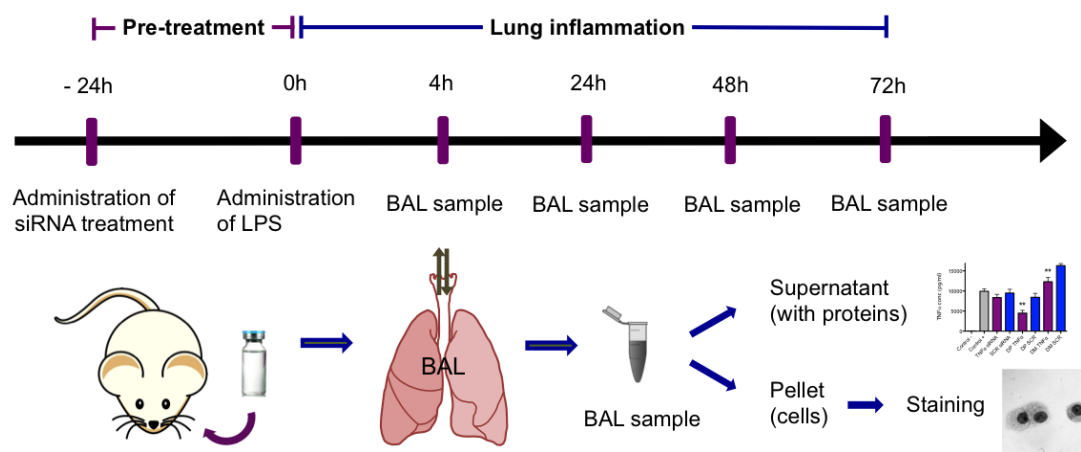


Figure 2. Schematic overview of the timeline in the animal experimental model and the subsequent sample analysis.

#### 2.10.4 Cell counting and differentiation

The total cell number in each lavage was counted using KOVA Glasstic hemocytometer slides, (KOVA international, Amsterdam, The Netherlands). For each animal, the ratio between neutrophils and macrophages (N/M ratio) was calculated based on counting a total of 300 cells.

#### 2.10.5 Protein quantification

Protein levels in the BAL were quantified using the Cytometric Bead Array - Mouse inflammation kit (BD biosciences), and the IL-6, IL-10, Interferon- $\gamma$  (IFN- $\gamma$ ) and TNF- $\alpha$  protein levels in the BAL were measured. BAL supernatants were stored at -20  $^{\circ}$ C and were used directly or diluted (1:3, v/v)

in assay diluent from the kit, and the samples were prepared following the instructions in the protocol of the kit. The BAL protein levels were finally quantified by flow cytometry using an Accuri C6) with 2000 ROI counts measured for each sample. All samples were prepared in duplicates and analyzed using the BD Accuri C6 software.

## 295 **2.11 Statistics**

Data reported for the cell studies are given as mean values  $\pm$  SD. Data reported for the *in vivo* studies are given as mean values  $\pm$  SEM. The *in vitro* and *in vivo* data were all based on independent replicates with each sample set consisting of samples prepared in different days. Statistical significance was confirmed by using the two-tailed and unpaired Student's t-test.

300 Statistical analyses were performed by using the student's t-test. The level of significance was set at  $p < 0.05$ .

## **3 Results and discussion**

### **3.1 Physicochemical characterization of dendrimers and dendriplexes**

All dendriplexes have a mean size between 120-190 nm and a PDI between 0.27-0.44 (Figure 3, A and B) whereas the hydrodynamic diameter of both dendrimers was around 3 nm (Table 1). Their polydispersity is consistent with what is reported in the literature for siRNA complexes self-assemble into larger aggregates<sup>31</sup>. No clear correlation between the N/P ratio and the resulting hydrodynamic diameter and PDI of the dendriplexes was observed. Similar size and PDI of DP and DM dendriplexes were measured. A positive zeta potential was observed for all dendriplexes, 310 indicating an overall positive surface charge (Figure 3C). The zeta potential increased as a function of N/P ratio due to the higher charge ratio resulting in better siRNA condensation and higher surface charge. Higher zeta potential values were generally observed for DP dendriplexes than for DM dendriplexes at all N/P ratios. This is related to the difference in pKa value of the two

dendrimers. DP and DM dendrimers have a pKa value of 8.1 and 7.1, respectively (Table 1).  
 315 Therefore at a pH of 7.4 in HEPES buffer, DP dendrimers are more ionized than DM dendrimers  
 resulting in higher positive zeta potential values.

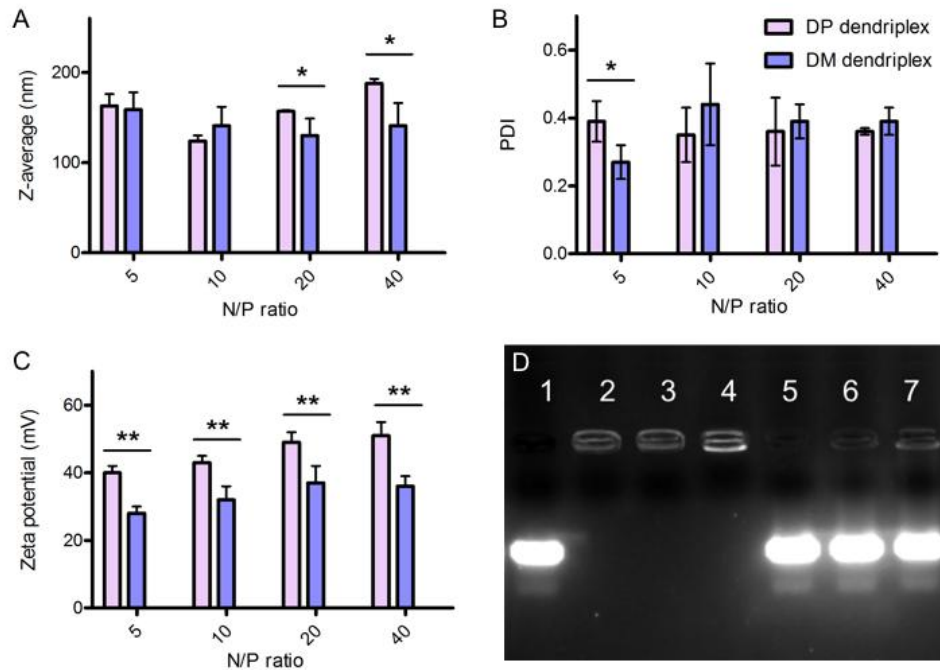


Figure 3. Z-average (A), polydispersity index (PDI) (B) and zeta potential (C) of DP and DM dendriplex aggregates prepared in HEPES buffer (10 mM, pH 7.4). Data points represent mean values  $\pm$  SD ( $n \geq 3$ ). Statistically significant differences between DP and DM dendriplexes are indicated:  $*p \leq 0.05$ ,  $**p \leq 0.01$ ,  $***p \leq 0.001$ . Agarose gel electrophoresis of dendriplex aggregates (0.9  $\mu$ g siRNA loading) (D). 1: Non-complexed siRNA; 2-4: DP dendriplex aggregates at N/P ratios of 5, 10, and 20, respectively, 5-7; DM dendriplex aggregates at N/P ratios of 5, 10 and 20, respectively.

325 Gel electrophoresis studies give an indication of the binding affinity between siRNA and the dendrimers. These studies show stronger binding between siRNA and dendrimers at higher N/P ratios for both DP and DM dendrimers confirming the zeta potential observations (Figure 3D). Binding with siRNA was substantially different for DP and DM dendrimers with DP dendriplexes retaining their siRNA, while DM dendriplexes mostly disassociated upon electrophoresis,  
 330

indicating stronger binding for DP dendriplexes. This result is again related to the difference in ionization of the dendrimers due to their different pKa values. As complexation is performed at a pH value slightly above the pKa value of DM dendrimers, only a few amine groups are charged and the binding is weaker than for DP dendrimers. Given the results obtained at different N/P ratios, biological studies were carried out at an N/P ratio of 5 to maximize the amount of siRNA associated to the dendriplexes while providing dendriplexes with comparable hydrodynamic size and siRNA binding affinity.

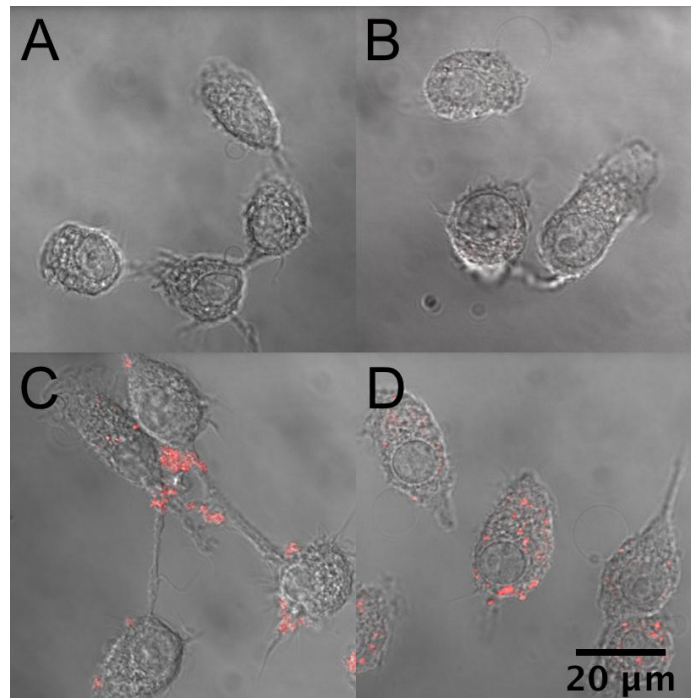
### 3.2 Cytotoxicity and cell uptake of dendriplexes

The cell viability was evaluated by measurement of the mitochondrial activity using the MTT assay on RAW 264.7 cells to determine the maximal tolerated concentration for further transfection experiments. Viability studies showed that dendriplexes prepared using the two different types of dendrimers possess significantly different toxicity profiles (Figure 4A). DM dendriplexes did not show any notable reduction in cell viability in the studied concentration range ( $IC_{50} > 15 \mu\text{M}$  siRNA). In contrast, DP dendriplexes exhibited a reduction in cellular viability as a function of siRNA concentration, with a calculated  $IC_{50}$  siRNA concentration of 470 nM, corresponding to a dendrimer concentration of 41  $\mu\text{g/ml}$ . A similar toxicity profile was observed for the non-complexed dendrimers (Figure S1). Also here, the DP dendrimers showed significantly higher toxicity compared with the DM dendrimers, which did not have any measurable toxicity. The higher toxicity of DP dendriplexes measured in this study could partly be related to their higher surface charge, or perhaps due to higher cell permeation and a higher degree of interaction with cellular components. The assessment of cytotoxicity again highlights the pronounced difference between the two types of dendrimers with only slightly different surface functional groups. The cytotoxicity measured for the DP dendriplexes ( $IC_{50} = 41 \mu\text{g/ml}$ ) is comparable to that observed for other cationic polymer-based transfection agents, *e.g.*, PEI ( $IC_{50} = 40 \mu\text{g/ml}$ ) and poly-L-lysine (PLL) ( $IC_{50} = 45 \mu\text{g/ml}$ )<sup>32</sup>. For all subsequent cell studies, siRNA concentrations lower than 100 nM,



dendriplexes showed a small amount of the siRNA internalization, while the majority of the siRNA was adsorbed on the surface of the cells (Figure 5C). However, cells incubated with DP dendriplexes showed internalization of siRNA in the cells with siRNA distributed within the cytoplasm (Figure 5D).

380 The images indicate that DP dendriplexes are mainly taken up by cells whereas DM dendriplexes mainly tend to adhere to the outer surface of the cell membrane as aggregates. This indicates better internalization of DP dendriplexes compared with DM dendriplexes, which also confirms the observations from the flow cytometry measurements. The higher uptake observed for the DP dendriplexes could be explained by their stronger positive charge and better stability. DM  
385 dendriplexes most probably dissociate in the cell culture medium before aggregating on the cell surface. These results are in agreement with the stronger binding observed for DP dendriplexes than for DM dendriplexes and possibly also their higher net surface charge, which has been shown in several studies to result in higher cellular uptake<sup>33-35</sup>. The cell uptake results could also explain the difference of toxicity observed between the two dendriplexes. Indeed constructs with high positive  
390 charge have been reported to result in some cytotoxicity<sup>34</sup>. As DM dendrimers lead to a lower internalization, the mitochondrial activity is less affected and the resulting viability measured by MTT-assay remains higher.



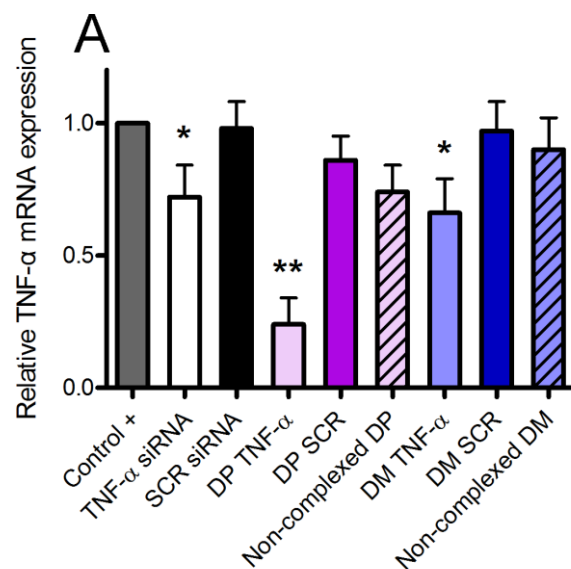
395 Figure 5. Representative image of the cellular uptake of dendriplexes in RAW 264.7 cells after 4 h of incubation. Overlay of a bright field and fluorescence image for untreated cells (A) and cells incubated with non-complexed siRNA (B), DM dendriplexes (C) and DP dendriplexes (D).

### 3.3 *In vitro* inhibition of TNF- $\alpha$ by dendriplexes in LPS treated macrophages

400 Cells treated with the dendriplexes containing TNF- $\alpha$  siRNA and subsequently activated with LPS were assessed at the mRNA level using RT-PCR (Figure 6). The relative TNF- $\alpha$  expression levels were lower for all TNF- $\alpha$  based samples compared with the corresponding scrambled siRNA samples. Non-complexed TNF- $\alpha$  siRNA showed 28 % inhibition, compared with the control, and a 26 % inhibition compared with scrambled siRNA, both statistically significant ( $p < 0.05$ ). The DM

405 dendriplexes with TNF- $\alpha$  siRNA showed 34 % inhibition, compared with the control, and 33% inhibition, compared with scrambled siRNA, which were statistically significant ( $p < 0.05$ ). The DP dendriplexes with TNF- $\alpha$  siRNA showed a rather substantial inhibition of 74 %, compared with the control, and a 50% inhibition, compared with scrambled siRNA, which were also statistically significant ( $p < 0.01$ ).

410 Dose-response studies were performed for DP (Figure 6B) and DM (Figure 6C) dendriplexes in the  
6-100 nM siRNA concentration range to assess the influence of the siRNA concentration on the  
gene inhibition, and ascertain that the observed effects were specific. For both DM and DP  
dendriplexes, the gene silencing was concentration-dependent. DM dendriplexes were shown to  
provide significant TNF- $\alpha$  knockdown from 50 nM siRNA and up while DP dendriplexes were  
415 shown to provide significant TNF- $\alpha$  knockdown from 25 nM siRNA and up. For both dendriplexes  
the highest dose (100 nM siRNA) was below the toxic level of dendriplexes for the cells. The  
transfection efficiency data correlates well with the observations from the cell uptake study, where  
it was demonstrated that DP dendriplexes result in higher cell internalization compared with DM  
dendriplexes and non-complexed siRNA. The higher silencing obtained with DP dendriplexes can  
420 thus be explained by their higher cell uptake and their higher stability and surface charge. Although  
DM dendriplexes did not indicate convincing cell uptake and structural stability, the nevertheless  
demonstrated a significant silencing of TNF- $\alpha$  expression. It was similar for the non-complexed  
siRNA, which showed a modest



425

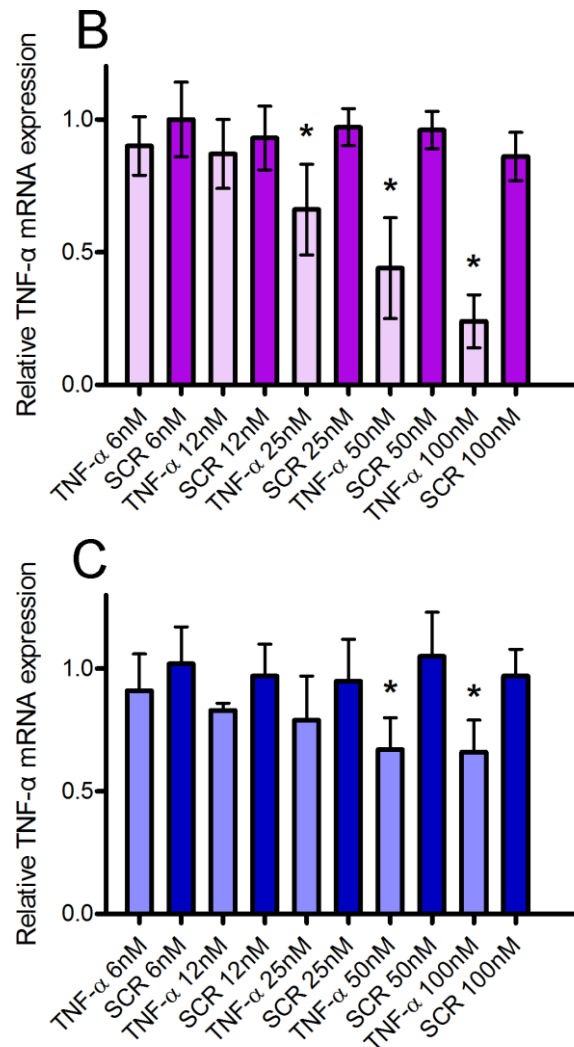


Figure 6. Dendriplex-mediated TNF- $\alpha$  mRNA silencing in RAW 264.7 cells. Normalization to LPS-treated cells (Control +) without siRNA was performed, and results denote the TNF- $\alpha$  mRNA expression level relative to transfection with negative control siRNA (referred to as scrambled (SCR) siRNA). (A) Samples corresponding to an siRNA concentration of 100 nM and an N/P ratio of 5, (B) Dose-dependent TNF- $\alpha$  mRNA silencing with DP dendriplexes, and (C) Dose-dependent TNF- $\alpha$  mRNA silencing with DM dendriplexes. Results denote the means  $\pm$  SD ( $n \geq 3$ ). Statistical significance: \*  $p < 0.05$ , \*\*  $p < 0.01$ .

435 but significant silencing of TNF- $\alpha$  expression at the highest concentration, despite low cellular uptake. This could indicate that only a small fraction of cellular siRNA uptake is sufficient to provide a silencing effect.

### 3.4 Modulation of the inflammation by dendriplexes in a murine acute lung injury model

An ALI model was used to assess the efficacy of the dendriplex formulations *in vivo*. LPS-induced  
440 ALI is considered one of the most important and applicable *in vivo* models to study molecular  
mechanisms and potential therapies for inflammation-associated lung injury as described<sup>36</sup>. In  
humans, once a patient develops lung injury, the best known strategy is supportive care<sup>37</sup>.  
However, many therapeutic agents have demonstrated a reduced efficacy, in part due the delay in  
initiating the therapy several days after the onset of lung injury<sup>37,38</sup>. This is why we intentionally  
445 decided to pretreat animals prior to administration of LPS, as a prophylactic treatment, and this is  
believed to represent the optimal therapeutic scheme.

The method for nasal instillation of the liquid suspensions was validated by administering a trypan  
blue solution to the mice and subsequently evaluating the deposition in the lungs and stomach. The  
lungs were entirely stained with trypan blue while the stomach did not show any dye, which  
450 indicates that most of the dye was delivered to the lungs (data not shown). The total cell count of  
the BAL indicates strong cell recruitment within 24 h after LPS challenge and is subsequently  
reduced as seen in the following time points (Figure S2A). The same trend was observed for the  
neutrophil-to-macrophage (N/M) ratio where neutrophil recruitment could be measured already  
after 4h. This also highlights that the majority of the subsequent cell recruitment observed occurs  
455 from the neutrophils (Figure S2B). Similar observations were made in other studies using intranasal  
instillation and LPS to assess therapeutic efficacy<sup>39,40</sup>

The cytokine profiles measured in the BAL after LPS challenge showed that the TNF- $\alpha$  levels  
(Figure S3) are very high 4 h after the animals are challenged with LPS and subsequently decrease  
over the next 3 days until they return to normal levels (32 pg/ml) after 7 days. A large increase was  
460 also observed for IL-6, IFN- $\gamma$  and IL-10, for which the cytokine levels in the lungs were either  
sustained (IL-6, IL-10) or increased progressively (IFN- $\gamma$ ), and for the latter maximum levels were  
reached at day 3 after LPS challenge, followed by a decrease to normal levels at day 7. Additional

inspection of the mice showed a significant reduction in weight (approx. 10%) and lack of grooming in the first three days following LPS challenge (data not shown).

465 Cytokine levels were compared for mice treated with LPS (Control +) and mice treated with non-complexed dendrimers in solution, as well as untreated mice (Control -) and were evaluated in order to assess the potential inflammatory response of the non-complexed dendrimers. Both dendrimers showed a small response for TNF- $\alpha$ , which was minor compared with the effect of LPS, yet significantly higher than the negative control, meaning that the dendrimers resulted in a small  
470 inflammatory up-regulation (Figure S4A). No visible effect was observed for IL-6 and IFN- $\gamma$  relative to the negative control (Figure S4A and S4B). However, both dendrimers experienced a slight increase in their IL-10 levels compared with the negative control indicating a small anti-inflammatory response by the dendrimers (Figure S4D).

The total BAL cell count was assessed for the different treatment conditions at 4 and 72 hours after  
475 LPS challenge. The cell population was not significantly different after 72 h (Figure S5A). The N/M ratio of the BAL for the different treatment conditions at 72 after LPS challenge was also assessed (Figure S5B). It was shown that the N/M ratio was lower for animals receiving a treatment containing anti-TNF- $\alpha$  treatment, although the differences in N/M ratio were not statistically significant. Yet, this could indicate a higher relative neutrophil recruitment for the positive control  
480 than for treated animals, which could also indicate a lower level of inflammation in the treated animals. Cytokine levels in the BAL were measured at different time points (4 and 72 h) after siRNA pre-treatment followed by LPS challenge. The siRNA dose was administered, based on previous pulmonary siRNA delivery studies (0.6-3 mg/kg siRNA administered)<sup>41-43</sup>, to ensure a sufficient level to observe a potential therapeutic effect. An siRNA dose of 2 mg/kg was chosen.  
485 The TNF- $\alpha$  protein levels measured 4 h after LPS challenge (Figure 7A) show that all treatments containing TNF- $\alpha$  siRNA resulted in a reduction in the TNF- $\alpha$  expression, compared with the corresponding treatments containing scrambled siRNA. The strongest inhibition was observed for DP TNF- $\alpha$  (55 %) compared to non-complexed TNF- $\alpha$  siRNA (17 %). The specificity of this

inhibition was demonstrated by the weakest effect of the scrambled siRNA delivered either non-  
490 complexed or by dendriplexes. DM TNF- $\alpha$  showed a slight increase in the TNF- $\alpha$  protein  
expression level, compared with the positive control confirming the lack of efficiency of these  
dendriplexes as shown *in vitro*.

Measurements of other cytokine levels show that the TNF- $\alpha$  based siRNA also has an influence on  
these, which is expected, as their regulation is interdependent. Significantly increased IL-10 protein  
495 levels were observed for DP TNF- $\alpha$  (18 fold increase, Figure 7D) compared with the positive  
control at 4 h after LPS administration. In contrast, the DM dendriplexes did not affect the BAL IL-  
10 level. This indicates that the DP TNF- $\alpha$  results in an anti-inflammatory response immediately  
after administering LPS. A substantial increase in the IL-6 protein secretion was observed for DP  
TNF- $\alpha$  (four-fold increase) compared with the positive control at 4 h after LPS administration  
500 (Figure 7C). The influence of non-complexed DP dendrimer on the cytokine expression was  
investigated by administering non-complexed DP dendrimer with a subsequent LPS challenge  
(Figure S6). It was observed, 4 h after LPS administration, that the non-complexed DP dendrimer  
resulted in an increase in IL-6 and IL-10, much lower than the secretion due to DP TNF- $\alpha$  and  
without any change in the production of TNF- $\alpha$ . The same trend is observed with scrambled-  
505 associated dendriplexes. If an increase in IL-10 results from anti-inflammatory effects, IL-6 should  
be downregulated as this is the case for TNF- $\alpha$ . We believe that IL-6 upregulation is due either to  
DP or to the specific sequence of siRNA, or both. Many authors have demonstrated that IL-6 in the  
murine LPS-induced lung injury model displays anti-inflammatory properties<sup>44,45</sup> and could  
contribute to reducing TNF- $\alpha$  to a certain extent as this was demonstrated on the same model after  
510 intratracheal administration of IL-6<sup>46</sup>. Although TNF- $\alpha$  and IL 6 return to very low levels 72 h after  
LPS challenge (Figure 8A and C), DP TNF- $\alpha$  siRNA still induces a strong inhibition of 44% for  
TNF- $\alpha$  compared with the positive control, much higher than non-complexed TNF- $\alpha$  siRNA or DM  
TNF- $\alpha$ . This sustained efficiency, three days following the onset of lung inflammation, suggests a

clear and efficient silencing effect provided by the siRNA. At 72 h, IL-6 levels had decreased for  
515 both DP-TNF- $\alpha$  and scrambled associated dendriplexes (Figure 8C).

Finally, IFN- $\gamma$ , a pro-inflammatory cytokine, was slightly reduced for mice treated with DP  
dendriplexes and non-complexed siRNA compared with the positive control at 4-h after LPS  
administration but not in a significant manner, which is normal since the kinetics of secretion of  
IFN- $\gamma$  is slowed down compared to the other cytokines (Figure 7 D). The overall trend of the  
520 cytokine levels indicates an anti-inflammatory effect of DP TNF- $\alpha$  compared with the positive  
control, induced by the effective transfection with anti-TNF- $\alpha$  siRNA. Unlike observations made at  
4 h, a considerable inhibition of IFN- $\gamma$  levels was observed for dendriplexes compared with the  
positive control and compared with non-complexed siRNA (Figure 8B). Also a ten-fold increase in  
the IFN- $\gamma$  levels was observed from 4 h to 72 h following LPS challenge whereas all other  
525 cytokines studied decreased in their levels over the same period.

From the *in vivo* assessment of the performance of the siRNA-loaded dendriplexes it can be  
established that the DP dendriplexes provided a more efficient silencing of TNF- $\alpha$  as well as a  
better anti-inflammatory regulation of other cytokines involved, compared with DM dendriplexes  
and non-complexed siRNA. This correlates well with the findings from *in vitro* transfection studies  
530 where the same trend was observed. The superior performance of DP dendriplexes is explained by  
the better ability of DP dendrimers to form stable complexes with siRNA therefore leading to a  
higher internalization in macrophages, which plays a key role in the production of TNF- $\alpha$ , a strong  
proinflammatory cytokine.

535

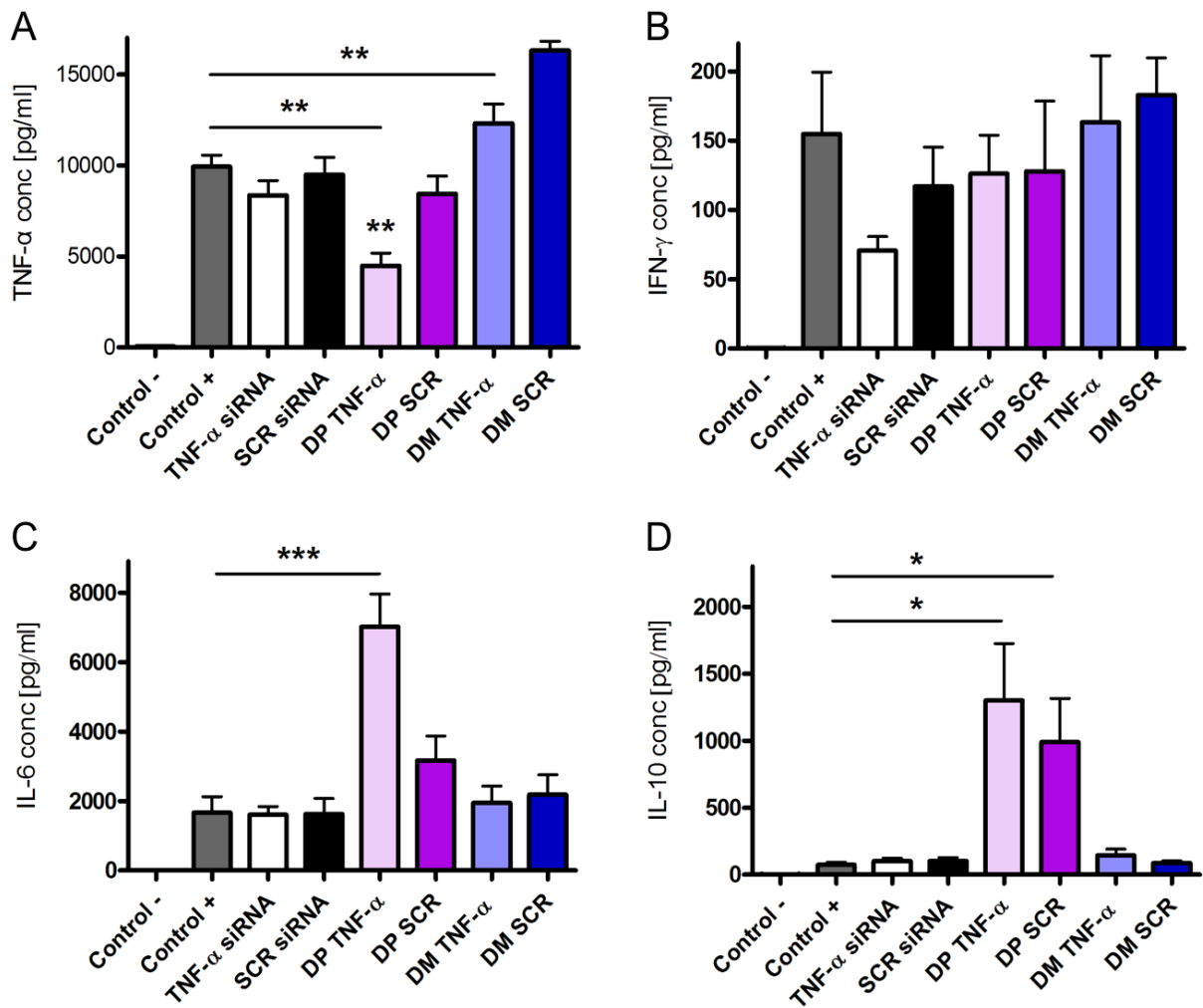


Figure 7. Cytokine concentration in BAL of mice challenged with LPS 24 h after administration of siRNA treatment, and euthanized 4 h after the LPS challenge, followed by extraction of BAL. Control - and Control + denote untreated and LPS-treated mice, respectively. Data points represent mean values  $\pm$  SEM.  $n \geq 5$ .

540 Statistical significance: \*  $p < 0.05$ , \*\*  $p < 0.01$ , and \*\*\*  $p < 0.001$ .

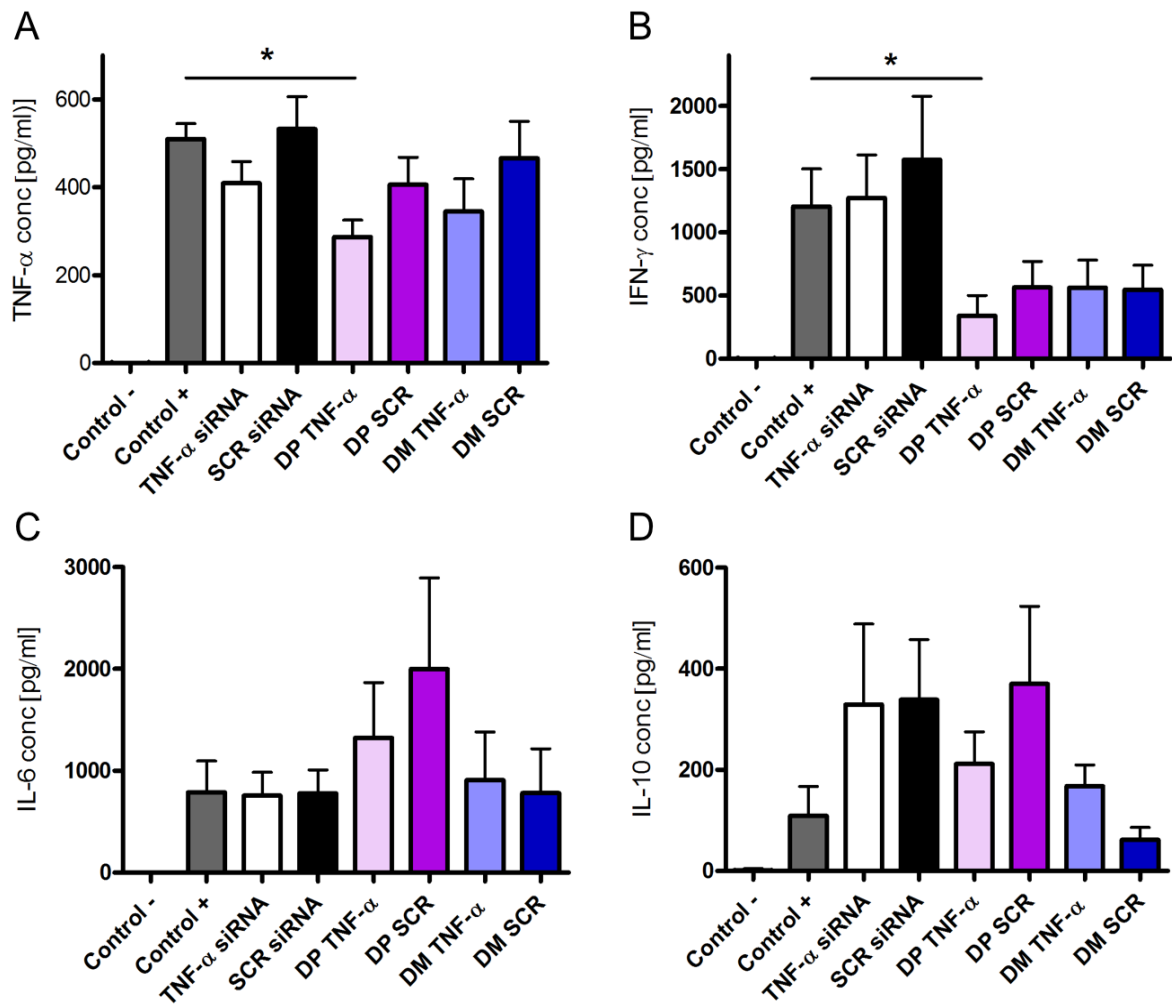


Figure 8. Cytokine concentration in bronchoalveolar lavage of mice challenged with LPS 24h after administration of siRNA treatment and euthanized 72h after LPS challenge for extraction of bronchoalveolar lavage. Control - and Control + denote untreated and LPS treated mice, respectively. Error bars show SEM.  $N \geq 5$ . Statistical significance: \*  $P < 0.05$ , \*\*  $P < 0.01$ , \*\*\*  $P < 0.001$ .

## 5. Conclusion

In this study, siRNA therapeutics was assessed for the treatment of acute inflammation, which was achieved both *in vitro* and *in vivo*. Major inhibition of TNF- $\alpha$  was obtained by means of a cationic phosphorous dendrimer containing pyrrolidinium and binding efficiently anti-TNF- $\alpha$  siRNA. The obtained dendriplexes are highly efficient in delivering siRNA to LPS-activated macrophages. After intranasal administration, TNF- $\alpha$  inhibition resulted in a strong anti-inflammatory effect as demonstrated by modulation of all other cytokines involved in the inflammation process.

555

### **Supporting Information**

- Procedure for dendrimer synthesis
- Primer sequences used for the RT-qPCR analyses
- Cell viability of RAW264.7 cells versus non-complexed dendrimers
- 560 - Bronchoalveolar lavage cell count and neutrophil-to-macrophage ratio in mice and following treatment and 72 hours after lipopolysaccharide challenge
- Cytokine concentrations in bronchoalveolar lavage of untreated mice or mice treated with non complexed dendrimers versus dendriplexes, 4h after intranasal challenge with phosphate buffer or lipopolysaccharide

### 565 **Acknowledgements**

The authors would like to thank the Danish Council for Independent Research (Grant No. DFF-12-131927) for financial support of this project. Further, Valérie Nicolas and Stéphanie Denis are acknowledged for their help with confocal microscopy and cell culture respectively. Authors would like to thank N. Szely, M. Beck-Broichsitter, J. Vergnaud and A. Biola-Vidamment for fruitful  
570 discussion. This study has been carried out with financial support from the Commission of the European Communities, Priority 3 “Nanotechnologies and Nanosciences, Knowledge Based Multifunctional Materials, New Production Processes and Devices” of the Sixth Framework Programme for Research and Technological Development (Targeted Delivery of Nanomedicine: NMP4-CT-2006-026668). The authors would also like to acknowledge the financial support provided by  
575 COST-European Cooperation in Science and Technology, to the COST Action MP1404: Simulation and pharmaceutical technologies for advanced patient-tailored inhaled medicines (Siminhale).

### **Disclaimer**

The content of this article is the authors’ responsibility and neither COST nor any person acting on its behalf is responsible for the use, which might be made of the information contained in it.

580

## References

- (1) Barnes, P. J. *Nat. Rev. Immunol.* **2008**, 8 (3), 183–192.
- (2) Lee, I.-T.; Yang, C.-M. *Mediators Inflamm.* **2013**, 2013, 791231.
- 585 (3) Wheeler, A. P.; Bernard, G. R.; Bernard, G.; al., et; Brochard, L. *Lancet (London, England)* **2007**, 369 (9572), 1553–1564.
- (4) Herold, S.; Mayer, K.; Lohmeyer, J. *Front. Immunol.* **2011**, 2 (NOV), 1–13.
- (5) O’Grady, N. P.; Preas II, H. L.; Pugin, J.; Fiuza, C.; Tropea, M.; Reda, D.; Banks, S. M.; Suffredini, a F. *Am. J. Respir. Crit. Care Med.* **2001**, 163, 1591–1598.
- (6) Patel, B. V.; Wilson, M. R.; O’Dea, K. P.; Takata, M. *J. Immunol.* **2013**, 190 (8), 4274–4282.
- 590 (7) GOLD Executive Committee. *Am. J. Respir. Crit. Care Med.* **2013**, 187 (4), 347–365.
- (8) Merkel, O. M.; Rubinstein, I.; Kissel, T. *Adv. Drug Deliv. Rev.* **2014**, 75, 112–128.
- (9) Nascimento, T. L.; Hillaireau, H.; Fattal, E. *J. Drug Deliv. Sci. Technol.* **2012**, 22 (1), 99–108.
- (10) Yin, H.; Kanasty, R. L.; Eltoukhy, A. A.; Vegas, A. J.; Dorkin, J. R.; Anderson, D. G. *Nat. Rev. Genet.* **2014**, 15 (8), 541–555.
- 595 (11) Lee, C. C.; MacKay, J. A.; Fréchet, J. M. J.; Szoka, F. C. *Nat. Biotechnol.* **2005**, 23 (12), 1517–1526.
- (12) Liu, X.; Rocchi, P.; Peng, L. *New J. Chem.* **2012**, 36 (2), 256.
- (13) Zhou, J.; Wu, J.; Hafdi, N.; Behr, J.-P.; Erbacher, P.; Peng, L. *Chem. Commun. (Camb)*. **2006**, No. 22, 2362–2364.
- 600 (14) Jensen, L. B.; Griger, J.; Naeye, B.; Varkouhi, A. K.; Raemdonck, K.; Schiffelers, R.; Lammers, T.; Storm, G.; de Smedt, S. C.; Sproat, B. S.; Nielsen, H. M.; Foged, C. *Pharm. Res.* **2012**, 29 (3), 669–682.
- (15) Dzitruk, V.; Szulc, A.; Shcharbin, D.; Janaszewska, A.; Shcharbina, N.; Lazniewska, J.; Novopashina, D.; Buyanova, M.; Ionov, M.; Klajnert-Maculewicz, B. *Int. J. Pharm.* **2015**, 485 (1), 288–294.
- 605 (16) Caminade, A.-M.; Majoral, J.-P. *Prog. Polym. Sci.* **2005**, 30 (3), 491–505.
- (17) Caminade, A.-M.; Majoral, J.-P. *Acc. Chem. Res.* **2004**, 37 (6), 341–348.
- (18) Spataro, G.; Malecaze, F.; Turrin, C.-O.; Soler, V.; Duhayon, C.; Elena, P.-P.; Majoral, J.-P.; Caminade, A.-M. *Eur. J. Med. Chem.* **2010**, 45 (1), 326–334.
- 610 (19) Fruchon, S.; Mouriot, S.; Thiollier, T.; Grandin, C.; Caminade, A.-M.; Turrin, C.-O.; Contamin, H.; Poupot, R. *Nanotoxicology* **2015**, 9 (4), 433–441.
- (20) Fruchon, S.; Poupot, M.; Martinet, L.; Turrin, C.-O.; Majoral, J.-P.; Fournié, J.-J.; Caminade, A.-M.; Poupot, R. *J. Leukoc. Biol.* **2009**, 85 (3), 553–562.

- 615 (21) Poupot, M.; Poupot, R.; Fournie, J.-J.; Portevin, D.; Fruchon, S.; Davignon, J.-L.; Davignon, C.-O.; Caminade, A.-M.; Majoral, J.-P.; Rolland, O. Google Patents August 2008.
- (22) Zheng, M.; Librizzi, D.; Kılıç, A.; Liu, Y.; Renz, H.; Merkel, O. M.; Kissel, T. *Biomaterials* **2012**, *33* (27), 6551–6558.
- (23) Sung, J. C.; Pulliam, B. L.; Edwards, D. A. *Trends in Biotechnology*. 2007, pp 563–570.
- 620 (24) Püschl, A.; Tedeschi, T.; Nielsen, P. E. *Org. Lett.* **2000**, *2* (26), 4161–4163.
- (25) Summerton, J.; WELLER, D. *Antisense Nucleic Acid Drug Dev.* **1997**, *7* (3), 187–195.
- (26) Launay, N.; Caminade, A.-M.; Majoral, J. P. *J. Organomet. Chem.* **1997**, *529* (1–2), 51–58.
- (27) Padié, C.; Maszewska, M.; Majchrzak, K.; Nawrot, B.; Caminade, A.-M.; Majoral, J.-P. *New J. Chem.* **2009**, *33* (2), 318–326.
- 625 (28) Ferretti, S.; Bonneau, O.; Dubois, G. R.; Jones, C. E.; Trifilieff, A. *J. Immunol.* **2003**, *170* (4), 2106–2112.
- (29) Giebelen, I. a J.; van Westerloo, D. J.; LaRosa, G. J.; de Vos, A. F.; van der Poll, T. *Shock* **2007**, *28* (6), 700–703.
- (30) Knapp, S.; Florquin, S.; Golenbock, D. T.; Poll, T. Van Der. *J. Immunol.* **2006**, *176* (5),  
630 3189–3195.
- (31) Conti, D. S.; Brewer, D.; Grashik, J.; Avasarala, S.; da Rocha, S. R. P. *Mol. Pharm.* **2014**, *11* (6), 1808–1822.
- (32) Wang, Y.; Kong, W.; Song, Y.; Duan, Y.; Wang, L.; Steinhoff, G.; Kong, D.; Yu, Y. *Biomacromolecules* **2009**, *10* (3), 617–622.
- 635 (33) Chung, T.-H.; Wu, S.-H.; Yao, M.; Lu, C.-W.; Lin, Y.-S.; Hung, Y.; Mou, C.-Y.; Chen, Y.-C.; Huang, D.-M. *Biomaterials* **2007**, *28* (19), 2959–2966.
- (34) Fröhlich, E. *Int J Nanomedicine* **2012**, *7*, 5577–5591.
- (35) He, C.; Hu, Y.; Yin, L.; Tang, C.; Yin, C. *Biomaterials* **2010**, *31* (13), 3657–3666.
- (36) Chen, H.; Bai, C.; Wang, X. *Expert Rev Respir Med* **2010**, *4*, 773–783.
- 640 (37) Levitt, J. E.; Matthay, M. a. *Crit. Care* **2012**, *16* (3), 223.
- (38) Litell, J. M.; Gong, M. N.; Talmor, D.; Gajic, O. *Respir. Care* **2011**, *56* (10), 1546–1554.
- (39) Poynter, M. E.; Irvin, C. G.; Janssen-Heininger, Y. M. W. *J. Immunol.* **2003**, *170* (12), 6257–6265.
- (40) Szarka, R. J.; Wang, N.; Gordon, L.; Nation, P. N.; Smith, R. H. *J. Immunol. Methods* **1997**,  
645 *202* (1), 49–57.
- (41) Conde, J.; Tian, F.; Hernandez, Y.; Bao, C.; Cui, D.; Janssen, K.-P.; Ibarra, M. R.; Baptista, P. V; Stoeger, T.; de la Fuente, J. M. *Biomaterials* **2013**, *34* (31), 7744–7753.
- (42) Dahlman, J. E.; Barnes, C.; Khan, O. F.; Thiriot, A.; Jhunjunwala, S.; Shaw, T. E.; Xing, Y.;

- 650 Sager, H. B.; Sahay, G.; Speciner, L.; Bader, A.; Bogorad, R. L.; Yin, H.; Racie, T.; Dong,  
Y.; Jiang, S.; Seedorf, D.; Dave, A.; Singh Sandhu, K.; Webber, M. J.; Novobrantseva, T.;  
Ruda, V. M.; Lytton-Jean, A. K. R.; Levins, C. G.; Kalish, B.; Mudge, D. K.; Perez, M.;  
Abezgauz, L.; Dutta, P.; Smith, L.; Charisse, K.; Kieran, M. W.; Fitzgerald, K.; Nahrendorf,  
M.; Danino, D.; Tuder, R. M.; von Andrian, U. H.; Akinc, A.; Panigrahy, D.; Schroeder, A.;  
Koteliansky, V.; Langer, R.; Anderson, D. G. *Nat. Nanotechnol.* **2014**, 9 (8), 648–655.
- 655 (43) Kusumoto, K.; Akita, H.; Ishitsuka, T.; Matsumoto, Y.; Nomoto, T.; Furukawa, R.; El-Sayed,  
A.; Hatakeyama, H.; Kajimoto, K.; Yamada, Y.; Kataoka, K.; Harashima, H. *ACS Nano*  
**2013**, 7 (9), 7534–7541.
- (44) Inoue, K.; Takano, H.; Yanagisawa, R.; Sakurai, M.; Shimada, A.; Satoh, M.; Yoshino, S.;  
Yamaki, K.; Yoshikawa, T. *Int. J. Immunopathol. Pharmacol.* **2008**, 21 (3), 501–507.
- 660 (45) Inoue, K.-I.; Takano, H.; Yanagisawa, R.; Sakurai, M.; Shimada, A.; Morita, T.; Sato, M.;  
Yoshino, S.; Yoshikawa, T. *Immunopharmacol. Immunotoxicol.* **2007**, 29 (1), 63–68.
- (46) Bhargava, R.; Janssen, W.; Altmann, C.; Andrés-Hernando, A.; Okamura, K.; Vandivier, R.  
W.; Ahuja, N.; Faubel, S. *PLoS One* **2013**, 8 (5), e61405.

665

Table 1. Physicochemical properties of cationic phosphorous dendrimers

<b>Dendrimer</b>	<b>Surface group</b>	<b>Primary amines</b>	<b>MW (g/mol)</b>	<b>pKa</b>	<b>Hydrodynamic diameter (nm)</b>
DP	Pyrrolidinium	48	16188.11	8.1	2.7
DM	Morpholinium	48	16956.06	7.1	2.9